Please fill in the name of the event you are preparing this manuscript for.	SPE Virtual Improved Oil Recovery Conference to be held 25-29 April 2022
Please fill in your 6-digit SPE manuscript number.	SPE-209355-MS
Please fill in your manuscript title.	An unconventional approach to model a polymer flood in the Kalamkas oilfield

Please fill in your author name(s) and company affiliation.

Given Name	Surname	Company
Marat	Sagyndikov	Satbayev University
Randall	Seright	New Mexico Institute of Mining and Technology
Nauryzbek	Tuyakov	LLP KMG Engineering (Kazakhstan)

Abstract

This article describes the main features of an unconventional approach to model a polymer flood in the Kalamkas oilfield. This non-standard simulation method is based on specially performed inter-well tracer tests, step-rate tests, pressure fall-off tests, dedicated field studies, well monitoring, and lab analysis. Our approach excludes permeability reduction as a mechanism to provide more mobility reduction than expected from rheology measurements (resistance factor) and by improving the recovery during post-polymer water flooding (residual resistance factor). Evidence is presented to support this exclusion for real field applications. Additionally, our approach places a significant emphasis on history matching bottomhole pressures. Our effort accounts well for the decreased mobility of the injected polymer solution and increased rock permeability during a polymer flood. In contrast to most other simulation approaches to polymer flooding, our method incorporates open fractures during polymer injection and their impact on injectivity and sweep efficiency. A literature review (lab tests and field cases) and our laboratory and field studies confirm the validity of our approach and its advantages over other modern simulator modeling of polymer flooding. From viscosity measurements of back-produced polymer solutions from injectors and well tests (inter-well tracer tests, pressure fall-off tests, step rate tests), we proved that polymer flooding induces fractures or fracture-like features and consequently, the polymer solution flows through the fracture with increased injectivity proportional to a resistance factor. Also, incorporated are expectations during a brine post-flush and the absence of the residual resistance factor (i.e., equal to 1). Implementation of these concepts brings our model closer to reality for simulating polymer floods.

Introduction

This paper's reservoir model is related to the Kalamkas oil and gas field. The Kalamkas field, situated in the western part of Kazakhstan, was discovered in 1976 and brought on stream in 1979 according to the Field Development Project – FPD (Lebin and Ogay 1979). Oil and gas reservoirs were established in the Jurassic deposits. Reservoirs mainly consist of sandstones deposited in deltaic, fluvial, and shallow marine environments. Taking into account the difference between reservoir pressures and bubble point pressures (20-30 bar), predicted liquid production under the natural depletion, and other geological features, an FDP was designed with the following scenario:

- A uniform 9-spot pattern with 400-m well spacing.

- Well orientation – vertical.
- Water injection started from the beginning of the development.
- The voidage replacement ratio was typically 100-120%.
- The injected water was either produced Jurassic brine and Cretaceous water reservoir brine.
- The injection bottom hole pressure (BHP) was below the initially measured formation parting pressure (120-140 bar).
- Production BHP was not allowed to drop below the bubble point pressure (50-70 bar).

Oil reservoirs have a high layered permeability contrast (>4) and unfavorable water-oil mobility ratio (M>7), which jeopardizes uniform depletion and oil recovery. In contrast, high average formation permeability (>500 md) and relatively low reservoir temperature (40°C) attract the implementation of chemical enhanced oil recovery (EOR) methods, such as polymer flooding. In view of the low reservoir temperature, elevated mobility ratio, and high formation permeability, it was recognized that there is considerable potential for enhancing oil production by polymer flooding. The first pilot test was initiated September 2014 in two injectors in the West part of the field and the second in four injectors in the East part of the field, beginning March 2015 (Sagyndikov et. al 2018; 2022). The West pilot includes 2 injectors with a 9-spot pattern (red rectangle in **Fig. 1**) as projected in the FPD, and the East pilot includes 4 injectors (red square in Fig. 1) with an infilled 5-spot pattern. Based on the pilots' results, the East polymer project was extended to the existing 9-spot well patterns using 11 injectors (blue polygon in Fig. 1). The earliest 4 polymer injectors of the East pilot were returned to waterflooding. To account for interference from surrounding wells, it was decided to build larger sector models—for the West pilot Block V (green polygon) and the East - Block IV (yellow polygon), as shown in Fig. 1.

During the operation of polymer projects, well monitoring, dedicated field studies, lab analysis, inter-well tracer tests, and well tests (step-rate and pressure fall-off tests) were conducted. The results of these studies were used to build a conceptual polymer flood model. An unconventional approach to model the polymer flood will be shown in the successful example of the West pilot. To date, we are working on the East polymer model, and the results are not yet complete.

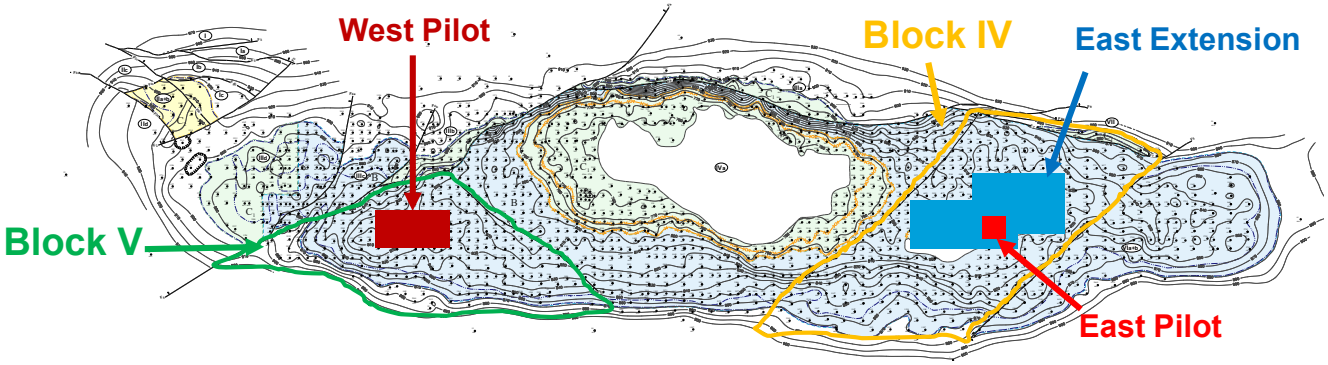

Fig. 1—Polymer flood project locations in the Kalamkas structural field map

Methodology

The overall approach to building the reservoir model is schematically shown in **Fig. 2.**

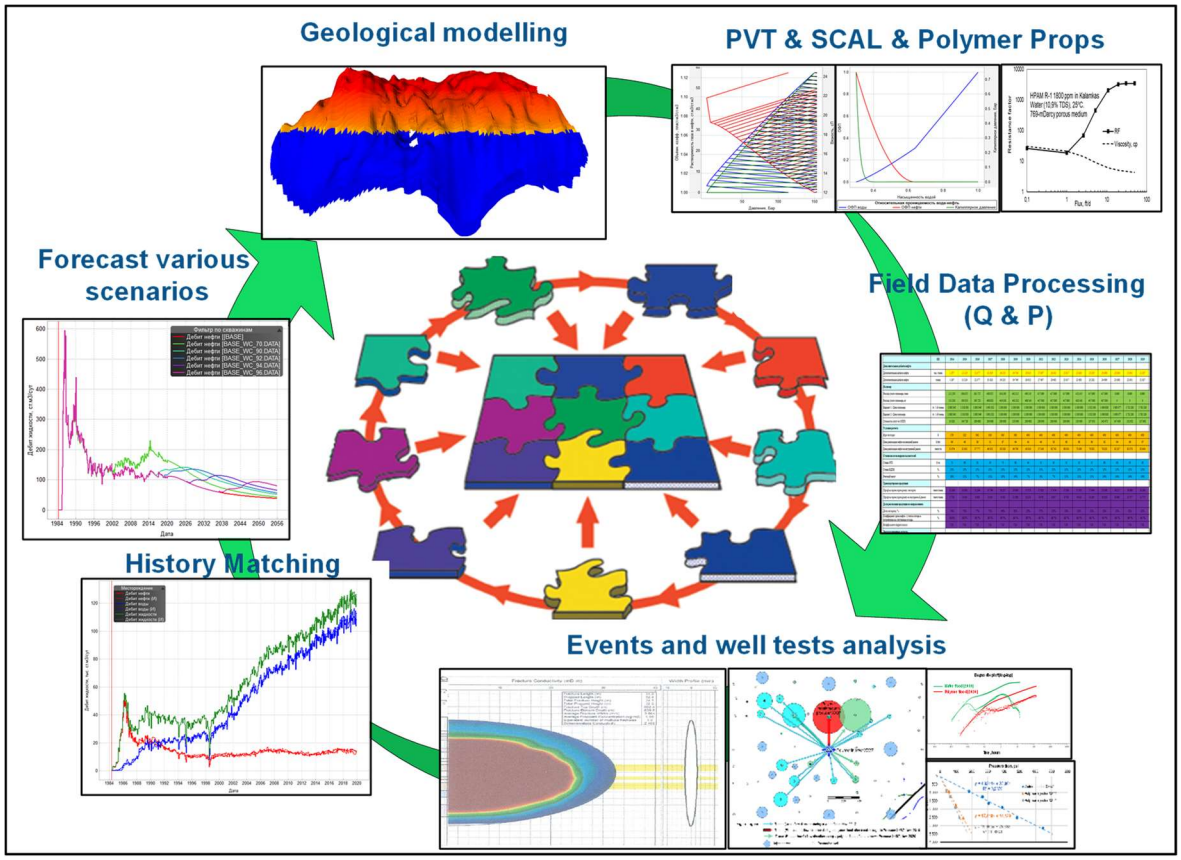

Fig. 2— Overall approach to build a reservoir model for a polymer flood

1. Geological modeling consists of structural modeling, creating a 3D grid, lithology and facies modeling, petrophysical modeling, oil reserves estimation, and finally initialization of the reservoir model. Grid dimensions were 50 m length, 50 m width, and 0.2 m height. Block V sector model included 1 439 340 cells (149x69x140), illustrated in **Fig. 3.**
2. Laboratory experimental (PVT, SCAL) results were systematically analyzed and existing models updated **(Figs. 4-5).**
3. Production and injection history were systematically investigated by analysis of production and injection logging tests (PLT&ILT). To accurately history-match reservoir performance, the upper reservoir was considered out-of-zone injection **(Fig. 6).**
4. Special core flooding experiments were conducted to estimate polymer rheology, retention, and mechanical degradation - providing key properties for the polymer flood and considered during setting polymer properties in the ".data" file.
5. For characterizing the production wells, we extensively analyzed well stimulation history (including hydraulic fracturing), well tests (pressure fall-off & step-rate tests), and inter-well tracer test results to build fractures or fracture-like features with proper orientation and configuration.
6. Water and polymer flood history matching emphasizing bottom-hole pressures (BHP).
7. Sensitivity analysis and forecast of various scenarios were performed to study the impact of polymer properties (viscosity, slug size, injection rate) on net present value – NPV.
8. We developed a correlation equation to estimate incremental oil production based on geological properties (layering, effective formation height, net to gross – NTG) and reservoir dynamic parameters (productivity index variation, depletion intensity, water cut).

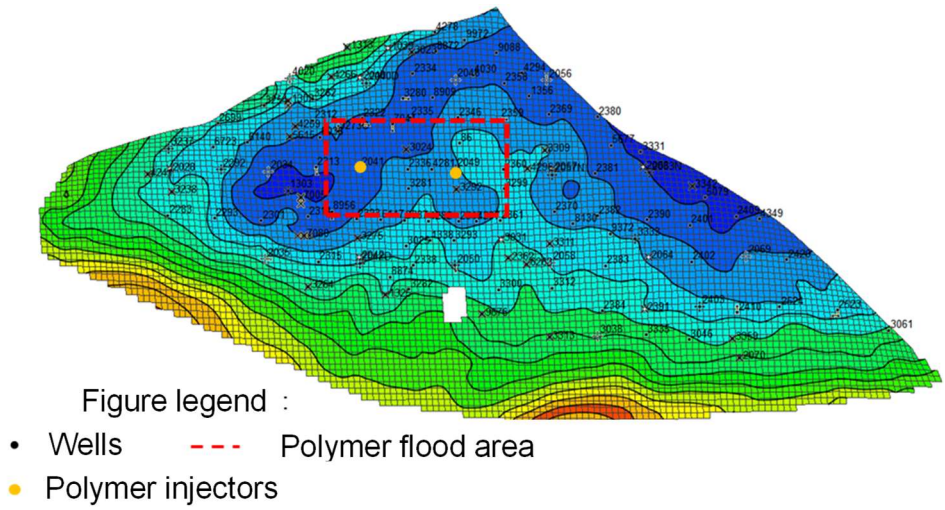

Fig. 3. Block V sector model which includes the West polymer flood pilot

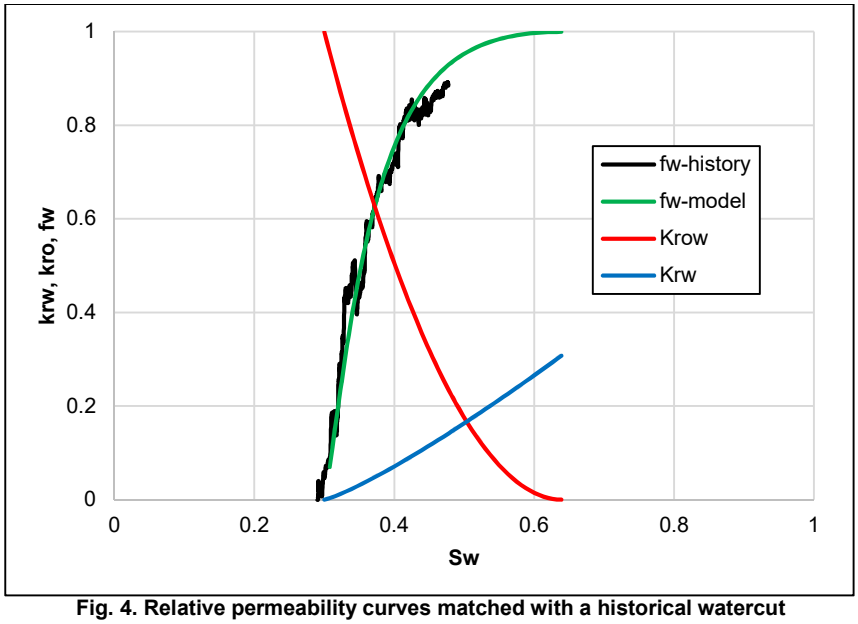

Fig. 4. Relative permeability curves matched with a historical watercut

Relative permeabilities analytically matched watercut history using a Buckley-Leverett function. As shown in Fig. 4, the actual watercut (black curve) is approximated well using a theoretical fractional water function (green curve). This approach saved significant time and resources.

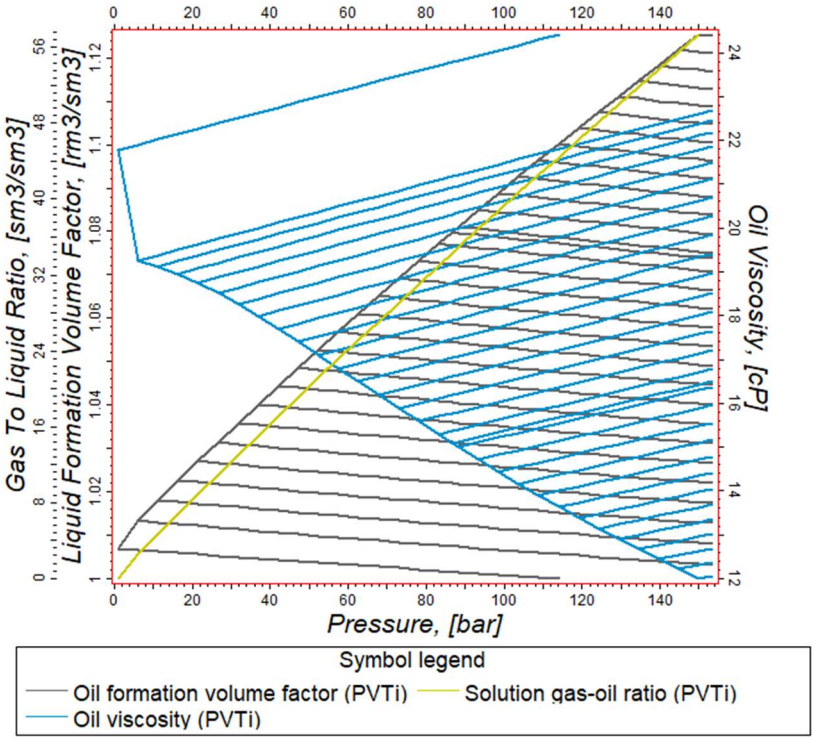

Fig. 5. Oil PVT properties used in the model

After a detailed analysis of all the formation samples for the reservoir, a PVT model was built in PVTi software using the oil and gas component compositions.

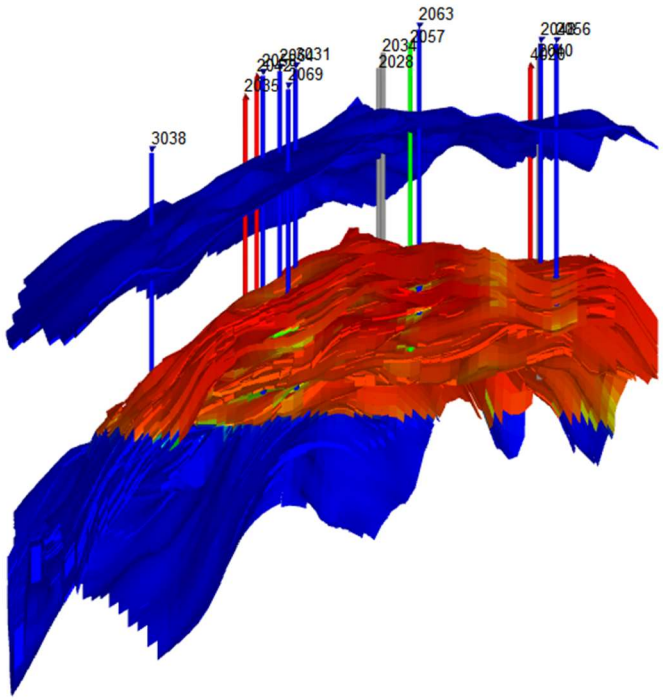

Fig. 6. Target reservoir and synthetic upper reservoir (considered out-of-zone injection)

The target reservoir model included 29 operated injection wells, with 15 of them registering out-of-zone injection at specific times. Total ineffective injection over 40 years was estimated at 1.5 million m^3 water. Our model considered these events to reproduce the real reservoir development history.

Polymer flood observed key aspects

Polymer Rheology in Porous Media or Resistance Factor. Resistance factor is defined as a ratio of injected water to polymer solution mobilities. Some researchers (Pye 1964; Smith 1970; Jennings et al. 1971; Hirasaki and Pope 1974) claimed that HPAM (the same type of polymer used in the Kalamkas project) solutions reduced mobility much more than expected from the solution viscosity. They suggested that the polymer substantially decreased permeability due to polymer adsorption and/or mechanical entrapment. This effect was often achieved during flooding experiments on short cores using freshly prepared HPAM solution. This permeability reduction behavior is considered in most modern simulators (e.g., Eclipse, tnavigator), including the model used for this study. In contrast, Seright et al. (2011) demonstrated that this mechanism is not practically achievable in field applications because HPAM high molecular species (which were responsible for permeability reduction) are filtered or destroyed at the injection sandface and will not propagate far into the reservoir. Consequently, deep in the formation where permeability >100 md, polymer solution are expected to provide mobility reduction proportional to the low shear rate viscosity measured in a rheometer. Thus, in a high-permeability formation like the Kalamkas field, polymer solution resistance factor or apparent viscosity in porous media is best represented by low-shear-rate viscosity measurements. In contrast, if polymer retention truly caused low mobility and permeability reduction, BHP values in polymer injectors would increase to high values. This effect has been demonstrated in our reservoir model, and the results show high BHP values were never observed in the Kalamkas field (Table 1). Thus, we excluded permeability reduction as a mechanism to provide more mobility reduction than expected from rheology measurements.

Case	Permeability reduction	Injector BHP, bar	History matching quality, +/- %
0 (history)		125.9	
1	1	123.6	-1.9
2	1.1	132.0	4.6
3	1.2	136.3	7.6
5	1.4	145.4	13.4
6	1.8	165.1	23.7
7	2	175.6	28.3
8	3	226.2	44.3
9	4	279.9	55.0

Table 1— Analysis of the effect of permeability reduction on the polymer injector BHP

Residual Resistance Factor – RRF. Residual resistance factor is defined as a ratio of water mobility before versus after a polymer flood. As mentioned in the Introduction section, the original four East pilot polymer injectors were returned to water injection after a long period of polymer flooding. The pilot is an infilled 5-spot with an average well spacing of 200-250 m, including 9 producers **(Fig. 7a).** The producers' post-polymer water injection performance has been extensively analyzed.

After the pilot started, liquid production of all producers were increased by changing downhole pumps. This action led to the first oil rate to increase, then stabilization, and later decline between March 2015 and February 2016. The polymer response started in August 2016 at 30% PV injected. This effect continued until the end of the project. As a result, the watercut decreased from 91% to 86%, and the oil rate increased by ~60%. When the polymer bank size reached 50% PV, injectors were returned to waterflooding. As shown in **Fig. 7b,** water injection led to a sharp (during the first month) water-cut increase from 86% to 91%, and oil rate decreased by at least 60% - i.e., oil production returned to the previous level before the polymer response.

As demonstrated in this field case for the Kalamkas high permeability conditions (>500 md), residual resistance factor is not significantly different from unity. It supports our conservative view for polymer-flood design, which assumes that resistance factor was approximated well using low-shear-rate viscosity

measurements and no permeability reduction. Thus, we suggest setting RRF in the simulator at 1. But even if the model assumes no permeability reduction, it could not reproduce the performance during post-polymer water injection—because of viscous fingering of the chase water through the polymer bank in the high permeable path. This effect has been experimentally proved by Seright (2017) and illustrated in **Fig. 8.**

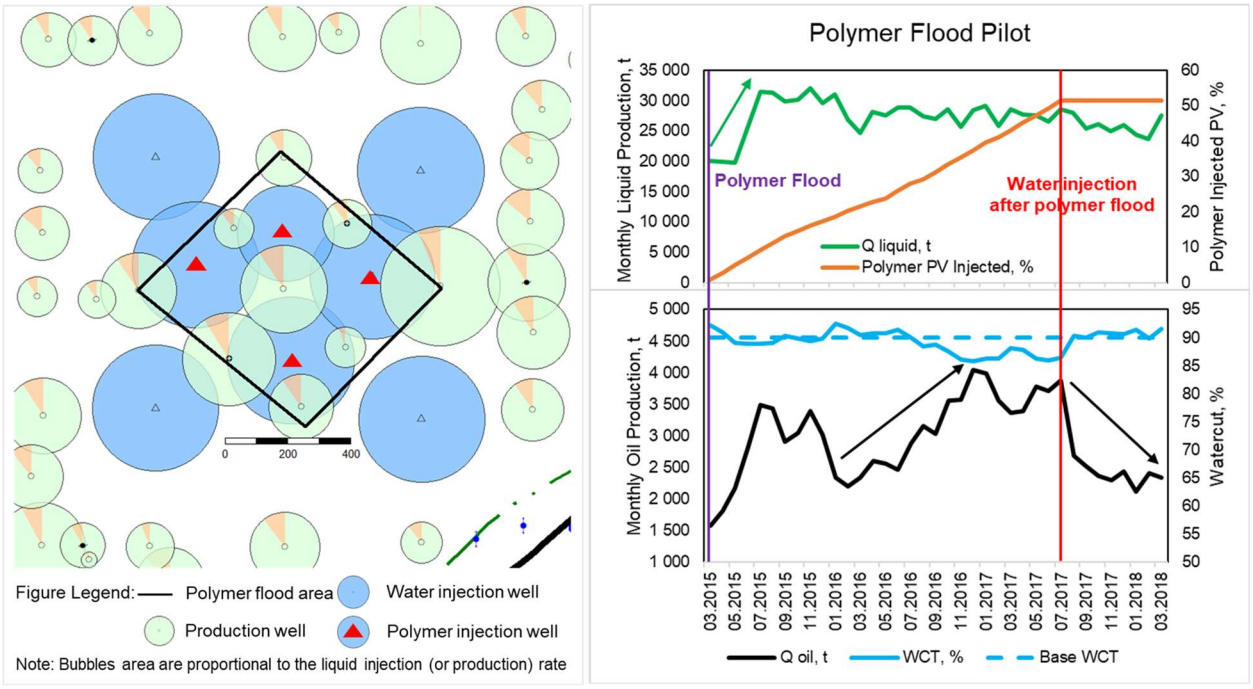

(a) (b)

Fig. 7- Polymer flood pilot area (a) and production response (b)

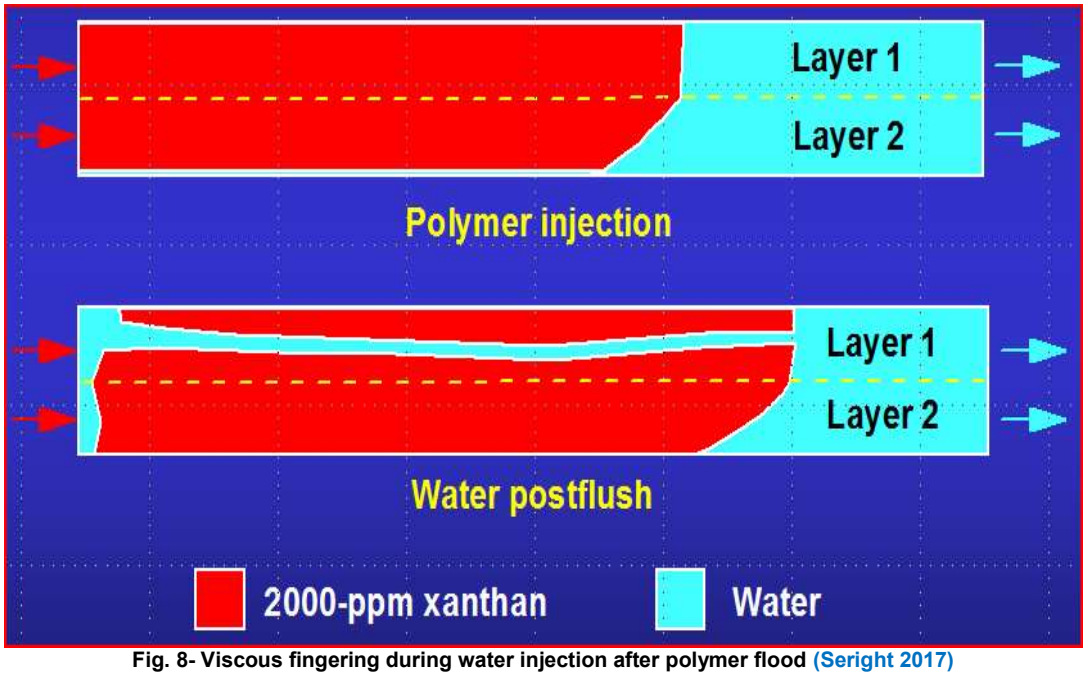

Fig. 8- Viscous fingering during water injection after polymer flood (Seright 2017)

The simulation scenario associated with a post-polymer chase waterflood (WF) is shown in **Fig. 9.** The blue curve show projections from the model during post-polymer chase water injection, while the green curve shows the projection for continued polymer injection. In this model, the switch from polymer to water injection began at the start of the blue curve (Feb. 2020). These projections suggest that a post-

polymer waterflood will maintain oil rates and water cuts that are significantly more desirable than associated with waterflooding alone (e.g., the red dashed curve). Additionally, the difference in oil production between continuing polymer flood (green curve) and returning to water injection (blue curve) is only 9.2%. Clearly, an economically rational scenario is a chase waterflood. However, as the East pilot demonstrated, oil rates are actually expected to return to the water flood base case after returning to water injection. Thus, considering the model's ability and real polymer flood physics, we suggest an accurate forecast for water chase flood rapidly returns to the waterflood base case line (red dashed curve).

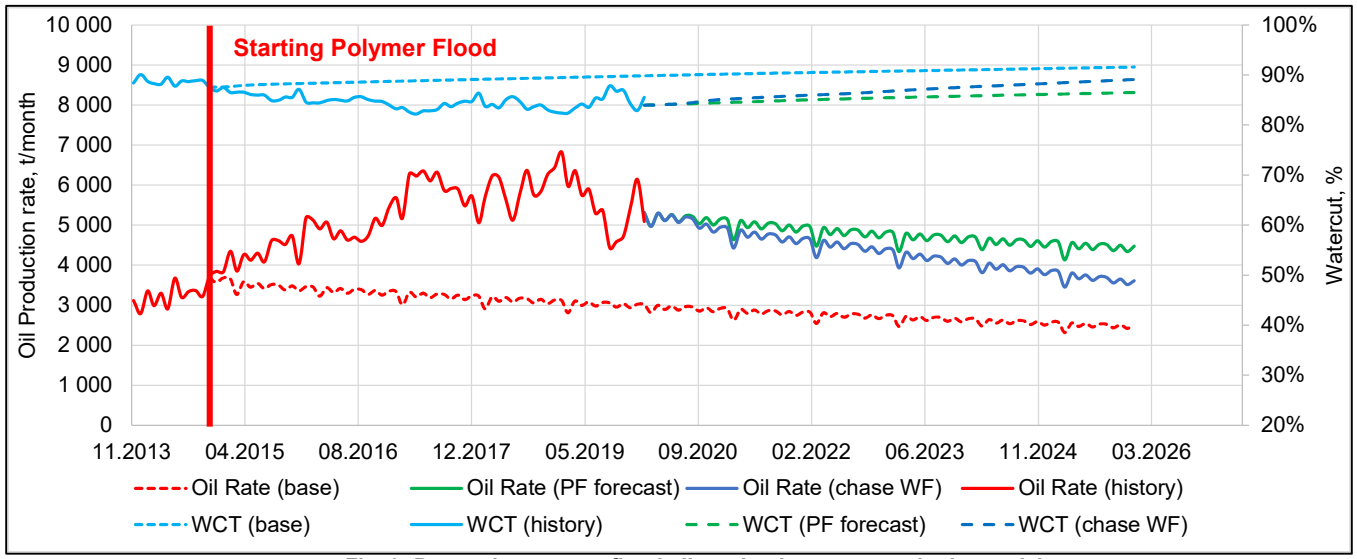

Fig. 9- Post polymer waterflood oil production response in the model

Inaccessible pore volume - IAPV. Considering uncertainties in laboratory studies to date and the high permeability condition of the Kalamkas field, we suggest IAPV should be set as zero during simulations. Previous work (Manichand and Seright 2014; Wang et al. 2020) demonstrated that is approach is appropriately conservative, and also most likely is correct/true. Simulation studies revealed that BHP and watercut response are not sensitive to IAPV values from 5% to 30%.

Polymer retention. Laboratory measurements of polymer retention were performed using a core plug from the target polymer-flooded reservoir. The core plug was chosen to represent the average permeability of the target reservoir. The rock absolute permeability was 380 md and porosity was 31.3%. The plug sample was cleaned with toluene, then saturated with formation water from the target reservoir., (This water was cleaned/filtered to remove oxidized products and suspended solids). The Kalamkas formation water contains 4 600-ppm calcium, 2 200-ppm magnesium, and has a total salinity of 98 700-ppm TDS. This water was used to prepare polymer solutions during the field polymer flood. The polymer used in the field and in this lab test was SNF Superpusher K-129, which is a partially hydrolyzed polyacrylamide (HPAM) with a molecular weight of approximately 14 million g/mol and a hydrolysis degree of approximately 17%. We used 1000, 1500, 2000 ppm HPAM solutions in our retention test.
After preparation and saturation with brine, we measured residual oil saturation, and then injected polymer solutions at a fixed rate (1 ft/D) at the reservoir temperature of 40ºC. Polymer concentrations were measured using the bleach method (API RP63 1990). The retention of each polymer slug injected was calculated using Equation (1), as recommended in API RP63 (1990):

$$R = \frac{W \times Ci - Y \times Cp}{M} \qquad (1)$$

where: R = retention, µg/g; W = weight of polymer injected, g; Ci = concentration of polymer solution injected, unit fraction; Y = weight of fluid produced and analyzed, g; Cp = concentration of polymer in the produced sample, unit fraction; M = bulk mass of the core, g. The retention test results are shown in **Fig. 10.**

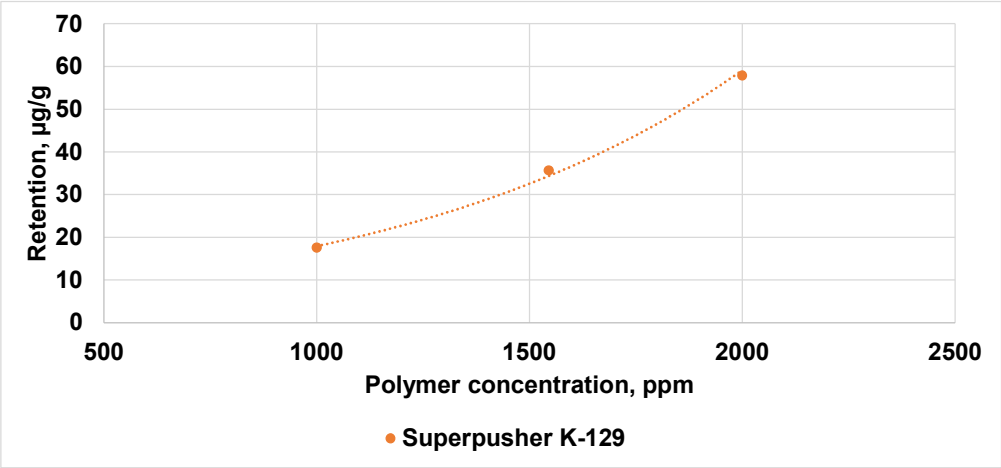

Fig. 10- Polymer retention test result

Polymer rheology. Polymer solution rheology was measured using a high-precision rheometer (Anton Paar MCR 502) at shear rates from 0-500 1/s, and reservoir temperature (40°C). As a solvent, we used formation water sampled from the field, which is used to prepare polymer solutions. **Fig. 11** plots rheology for 500-5000-ppm HPAM concentrations**.**

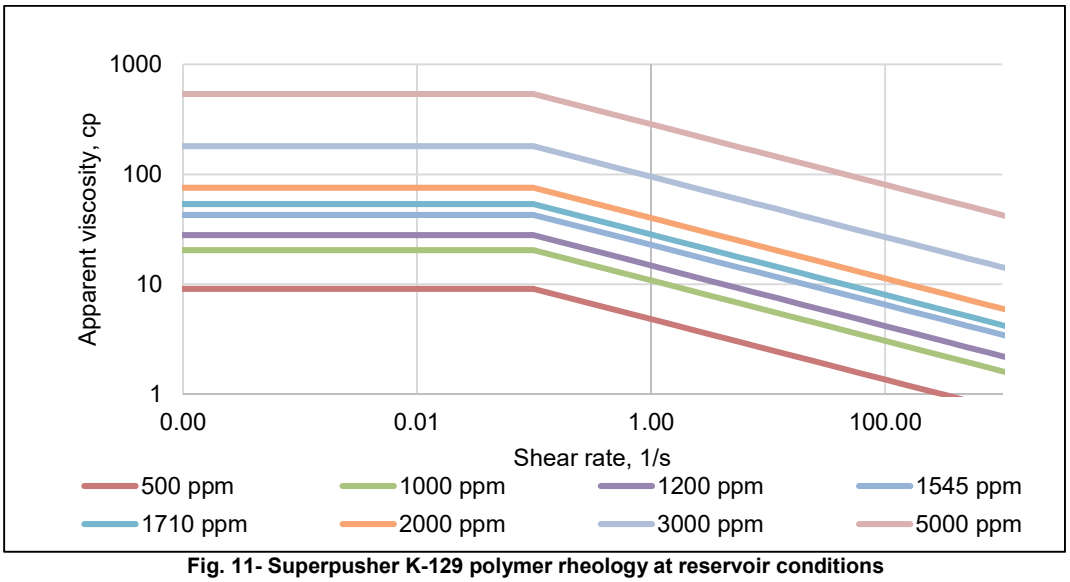

Fig. 11- Superpusher K-129 polymer rheology at reservoir conditions

Polymer induced fractures and their impact on the flood. Sagyndikov et al. (2022) provided Kalamkas field evidence to clarify the utility of near-wellbore fractures to promote injectivity and mitigate mechanical degradation of HPAM solutions. Well tests (step rate and pressure fall-off test) indicated that fractures were not open during water injection before polymer injection. In contrast, open fractures were confirmed during polymer injection using well tests and comparison of actual injectivities versus those calculated using the Darcy radial flow equation coupled with laboratory measurements of HPAM rheology in Kalamkas cores. In addition, viscosity measurements of sampled solutions from polymer injectors showed the absence of mechanical degradation. This finding provided further confirmation that polymer injection occurred above the formation parting pressure and that the injection area associated with the

fracture was large enough to ensure the stability of the solution. Thus our model assumed no mechanical degradation of polymer solutions and fracture flow near-wellbore. We used pressure fall-off test and inter-well test results to set fracture conductivity, half-length **(Fig. 12 and Table 2),** and orientation **(Figs. 13-14).**

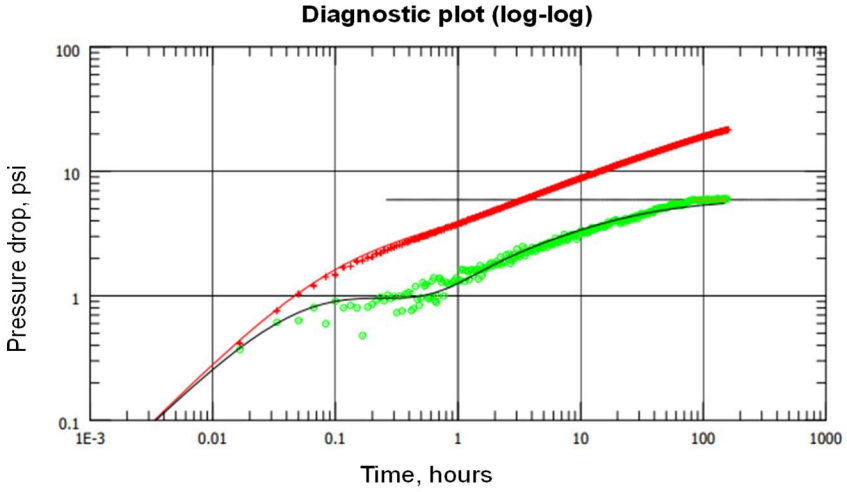

Fig. 12—Analysis of pressure fall-off test during polymer injection into Well XX41

No.	Parameter	Value	
		During polymer flood (2020)	During water flood (2014)
1	Perforation interval, Top-Bottom	795-826 m	795-826 m
2	Test duration, hours	163.5	
3	Well model	Vertical fractured finite conductivity	
4	Reservoir model	Homogenous	
5	Boundary model	Infinite	
6	Reservoir pressure, psi	1099	
7	BHP, psi	1794	N/A
8	Conductivity, md·m	1 260	
9	Average permeability, md	440.5	
10	Total skin	-6.16	
11	Geometrical skin	0.12	
12	Fracture half length, m	116	
13	Fracture conductivity, md·m	0.1E+6	
14	Injectivity index, bbl/(d·psi)	3.86	2.21

Table 2— Analysis of pressure fall-off test during polymer injection into Well XX41

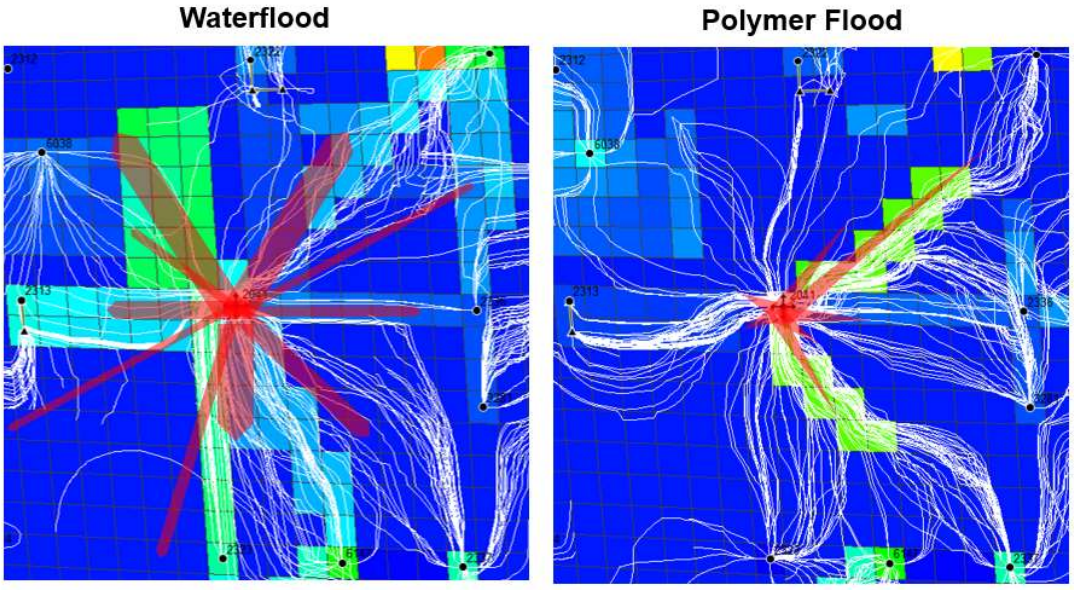

Fig. 13- Setting fracture configuration to the model based on well tests, Injector XX41

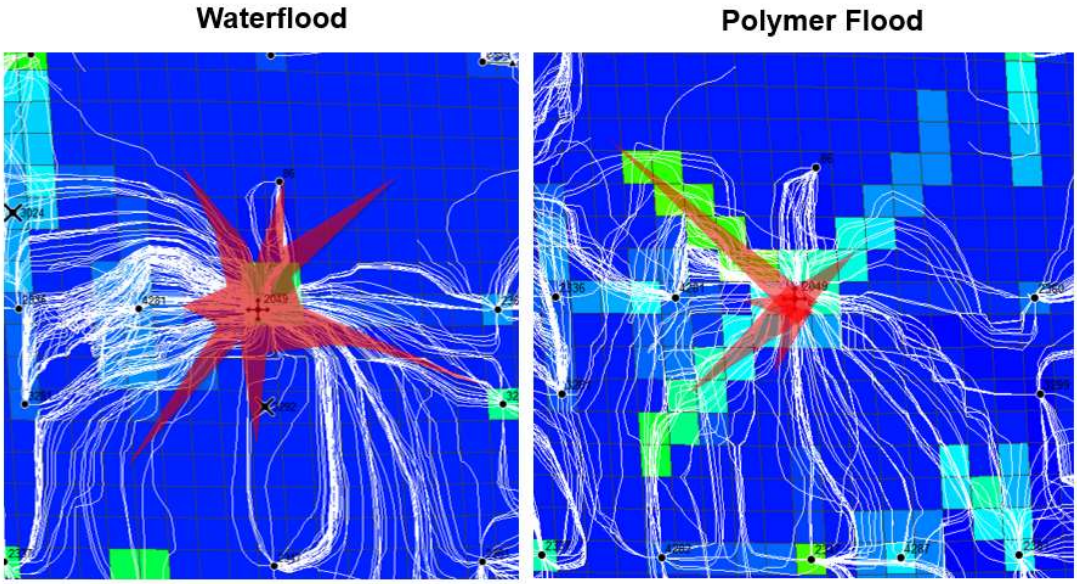

Fig. 14- Setting fracture configuration to the model based on well tests, Injector XX49

Injector Bottom-hole pressure (BHP) history matching. As shown on the left sides of **Figs. 15-16,** simulated BHP of the polymer injectors without fracture-like features shows a sharp increase, but this behavior is not observed in the field. In the previous section "Polymer induced fractures and their impact on the flooding", we demonstrated how to set fracture length and orientation. We used permeability as the main parameter to match the BHP. As a result, we obtained good history matching of BHP in polymer injectors, as shown on the right sides of Figs. 15-16.

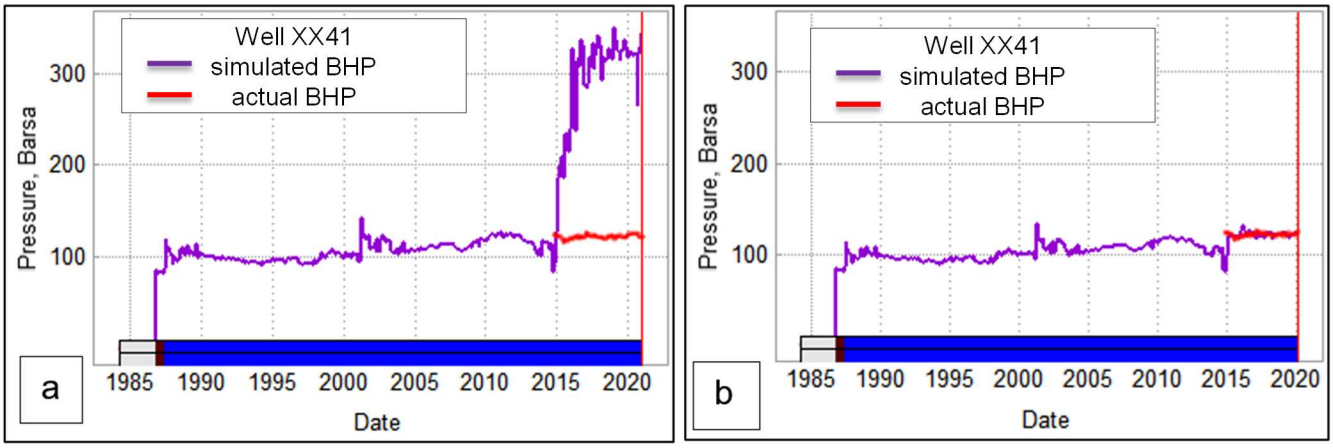

Fig. 15- BHP history matching for the Injector XX41 (left side: without fractures; right side: with fractures)

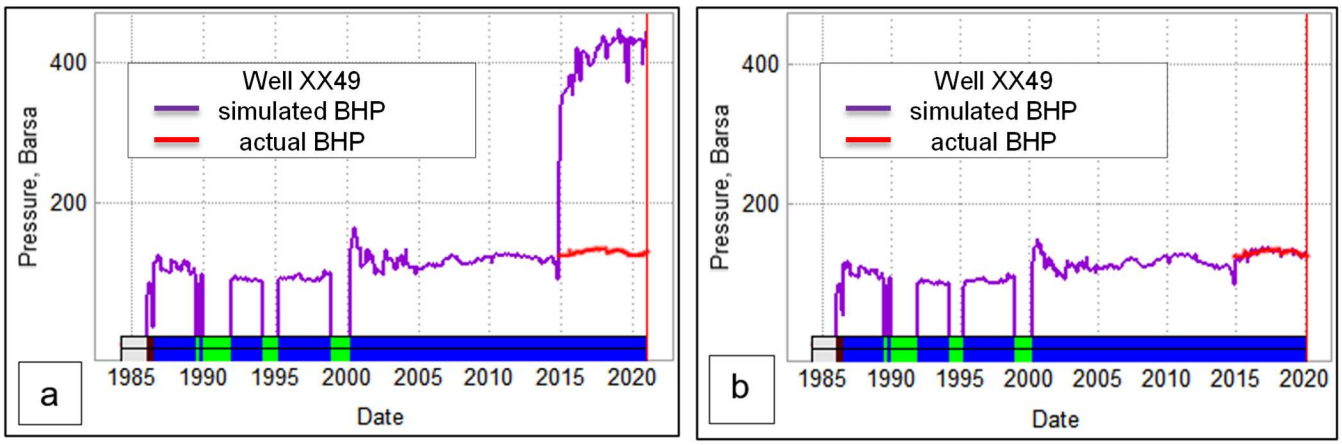

Fig. 16- BHP history matching for the Injector XX49 (left side: without fractures; right side: with fractures)

Results and discussions

Reservoir dynamic modeling shows satisfactory quality during the entire polymer flood period. Moreover, main parameters, such as liquid/oil rates and watercut, show minimum discrepancy. For example, at the end of the simulation period (Jan. 2020), the convergence on the oil rate was 99%, on the liquid rate – 98%, and watercut matches the actual 84% **(Fig. 17).**

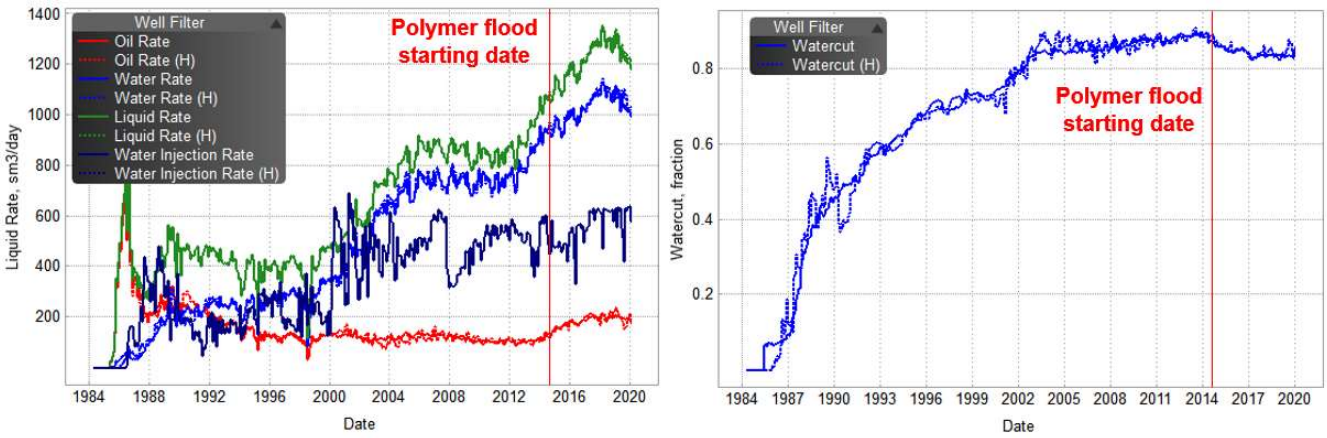

Fig. 17- Reservoir simulation history matching results

Model viability. We compared production forecast data and actual results for the 2020-2021 period to assess model viability **(Fig. 18).** The forecast shows good convergence.

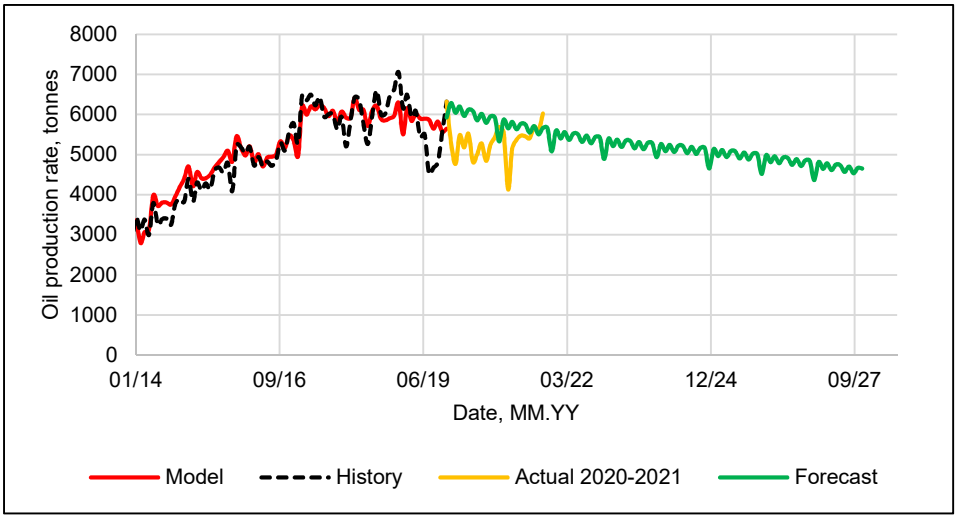

Fig. 18- Model forecast viability analysis

Optimization scenarios. After finishing the history matching work, we performed various simulation scenarios with different polymer concentrations, slug sizes, and injection rates. The forecast period was 10 years for all options, i.e., until 2029 **(Fig. 19-21).** As shown in Fig. 19, increasing polymer concentration (or viscosity) increases incremental oil production. However, extra expenditures related to additional polymer concentration lead to decreased net present value (NPV). In contrast, increasing the injection rate at a constant polymer concentration shows the same effect (Fig. 20). In another case (Fig. 21), assuming constant polymer consumption and making concentration & injection rate combination as variables, we can see that injection rate of 700-800 m^3/d and polymer concentration of 1.3-1.5 kg/sm^3 are the optimum ranges in terms of incremental oil production and NPV.

We also performed a simulation scenario with the optimum design (injection rate & polymer concentration) until ~110% pore volume (PV) was injected **(Fig. 22).** This scenario aims to show an economically feasible project life, with at least 60% of PV injected when the oil price is 40$ USD per one barrel (the most pessimistic case). In contrast, the most optimistic view (90$/bbl) shows close to 70% of PV injected. Therefore, consistent with Sheng (2015) and Seright (2017), our simulation studies reveal that polymer flood at oil price volatility is a long-term project that extends the field's economically feasible lifetime and enhances oil recovery.

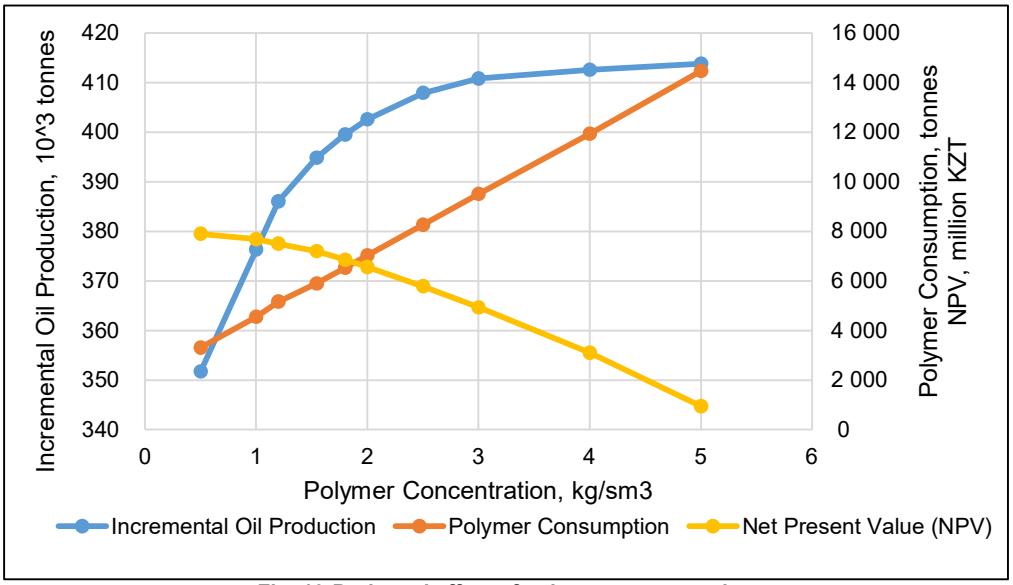

Fig. 19-Projected effect of polymer concentration

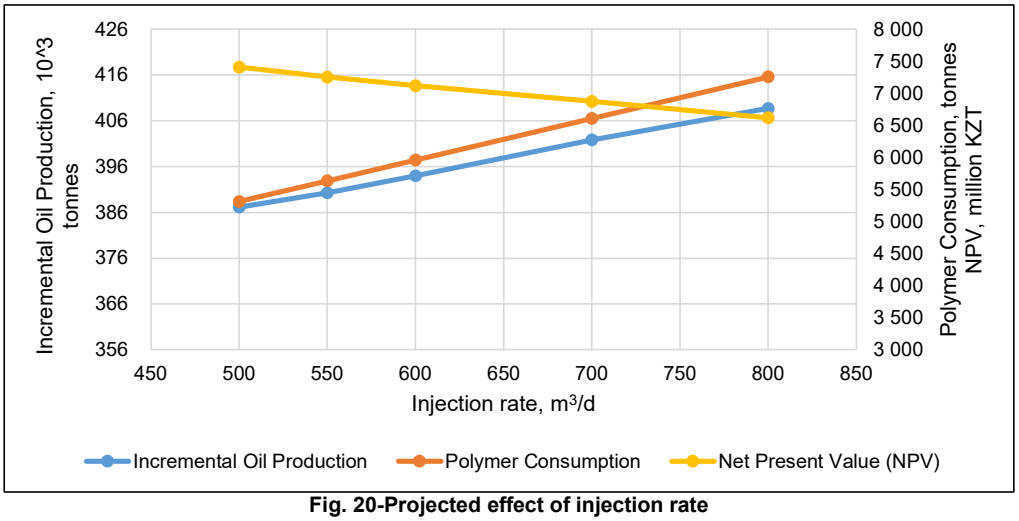

Fig. 20-Projected effect of injection rate

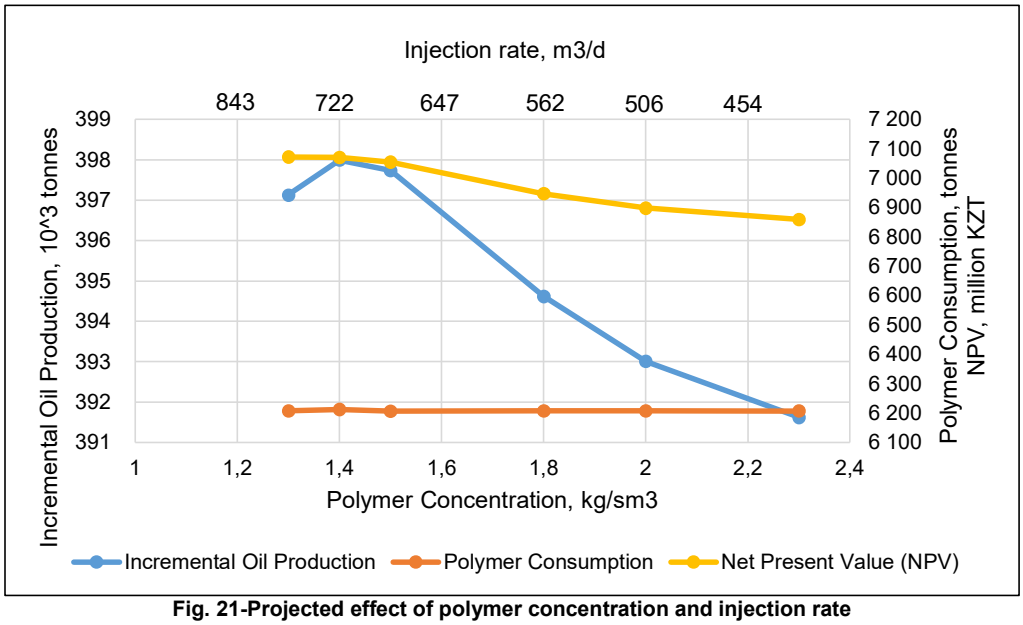

Fig. 21-Projected effect of polymer concentration and injection rate

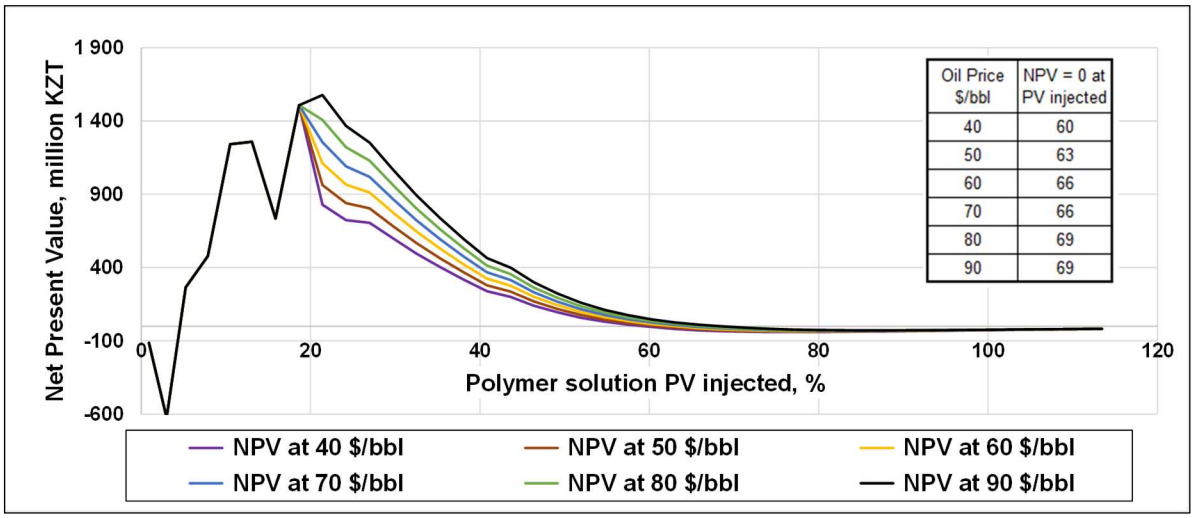

Fig. 22-Projected effect of oil price

Analytical equation to forecast a polymer flood. It is well known that the process of geological modeling and reservoir simulation requires enormous resources, including time, software, and electronic computing capacities. Additionally, the accuracy of the modeling depends on initial information and the quality of history matching. Therefore, to save time and accelerate the process of making a decision, we created five new synthetic areas **(Fig. 23)** with different geological properties (net-to-gross, layering, formation height) and current reservoir conditions (productivity indexes variation, depletion intensity, watercut). The simulation results for six areas (existing pilot and 5 new) are shown in **Fig. 24,** and the derived equation is shown in Equation **(2).** Equation (2) assumes that polymer concentration and injection rate are the same as in pilot wells pattern (XX41 and XX49).

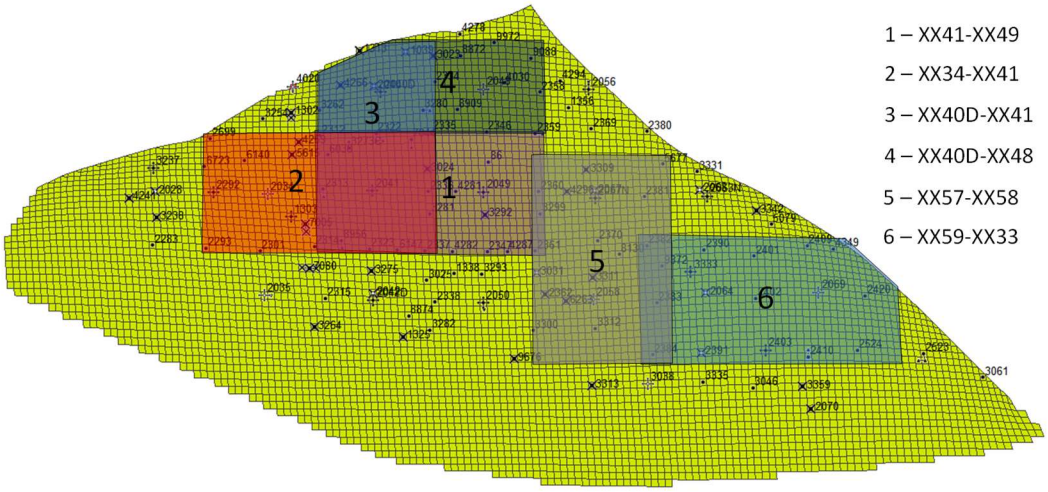

Fig. 23- Synthetic areas to simulate polymer flood at different geological and reservoir conditions

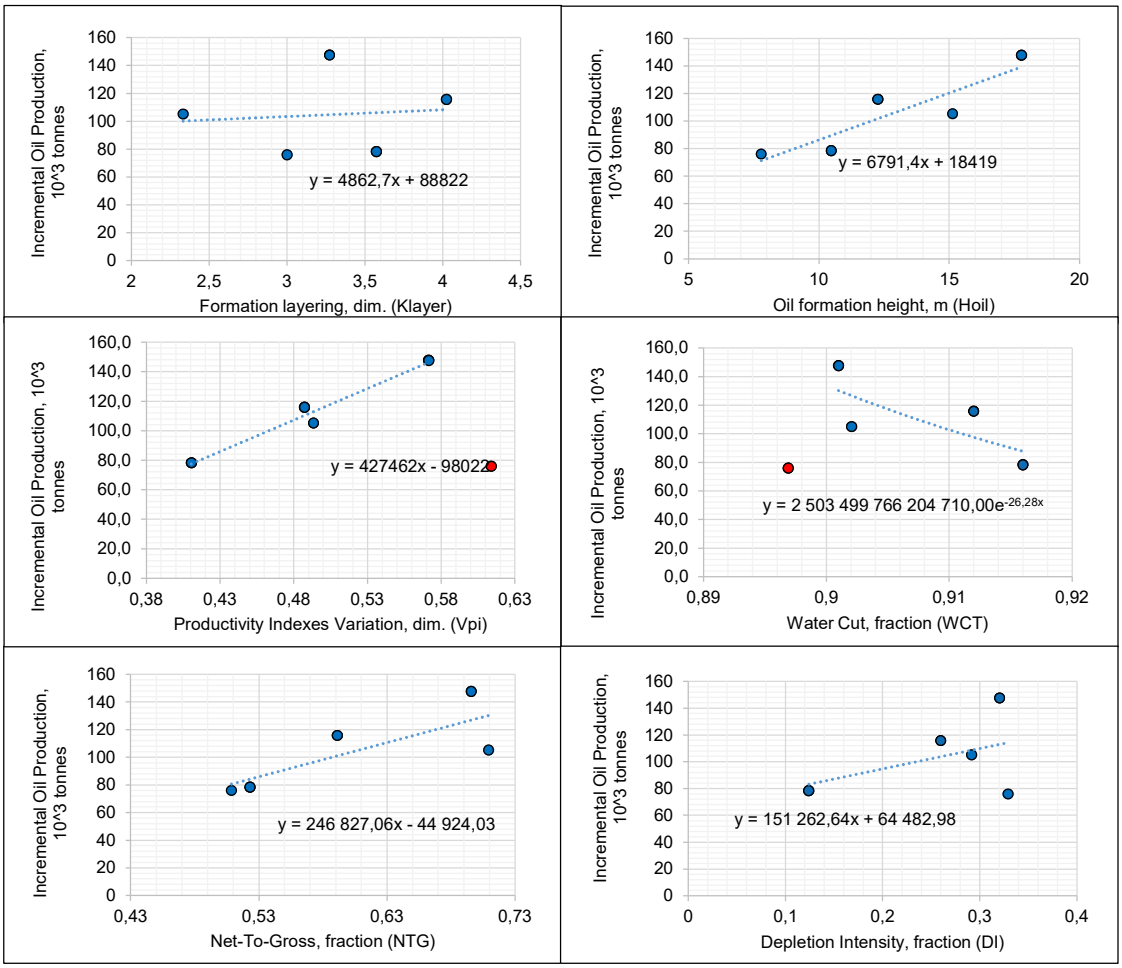

Fig. 24 – Analytical equation to forecast polymer flooding

$$IOP = (4862.7 * \boldsymbol{K}_{layer} + 6791 * \boldsymbol{H}_{oil} - 246827 * \boldsymbol{NTG} + 151262 * \boldsymbol{DI} + 427462 * \boldsymbol{V}_{\boldsymbol{PI}} + 2.50\text{E} + 15 * \boldsymbol{exp}(-2.63\text{E} + 01 * WCT)) + 28777 \div 6 \quad (2)$$

where: IOP = incremental oil production for 5 years, thousand tonnes; K layer = formation layering or compartmentalization index, dim.; Hoil = oil formation height, m; NTG = net-to-gross, fraction; DI = depletion intensity (defined as a difference between depletion of recoverable reserves and watercut), fraction; V pi = productivity indexes variation, dim.; WCT = watercut, fraction.

Comparison of the actual (field-observed) oil production with predictions from Eq. 2 matched reasonably well for most wells (shown by the blue circles in Fig. 24). In two wells (the red circles in Fig. 24), the match was not as good. This equation allows easy predictions in place of the expense and effort required for simulation. Of course, the development of empirical relations like Eq. 2 must be obtained individually for different reservoirs.

Conclusions

1. An unconventional method for modeling a polymer flood was developed that accounts for more realistic conditions that occur during polymer injection into vertical wells. These conditions include (a) fractured injection wells, (b) no mechanical degradation of injected polymer solutions, (c) no significant permeability reduction caused by the injected polymer, and (d) no polymer inaccessible pore volume. This model was applied in the Kalamkas oil field in Kazakhstan.

2. The model focuses on history matching of bottom-hole injection pressures and forecasts far better than conventional models that assume no fractures are present.
3. The model correctly predicts very rapid deterioration of water cuts and oil production rates after switching from polymer back to water injection—better than conventional models that assume as significant permeability reduction by the polymer.
4. An empirical equation matched oil production reasonably well for most wells in six areas of the Kalamkas oil field. This equation allows easy predictions in place of the expense and effort required for simulation.
5. Given oil-price volatility, feasibility studies reveal that our polymer flood should be a long-term project that extends the field's economic lifetime and enhances oil recovery.

Nomenclature

BHP = bottom-hole pressure, bar
Ci = concentration of polymer solution injected, unit fraction
Cp = concentration of polymer in the produced sample, unit fraction
DI = depletion intensity, fraction
f_w = fractional water curve or watercut, fraction
Hoil = oil formation height, m
IOP = incremental oil production for 5 years, thousand tonnes
k_{rw} = relative permeability by water, fraction
k_{ro} = relative permeability by oil, fraction
K layer = formation layering or compartmentalization index, dim.
M = bulk mass of the core, g
NPV = net present value, million KZT
NTG = net-to-gross, fraction
ppm = parts per million
PV = pore volume, %
R = retention, μg/g
S_w = water saturation, fraction
V pi = productivity indexes variation, dim.
W = weight of polymer injected
WCT = watercut, fraction
Y = weight of fluid produced and analyzed, g

Acknowledgments

The authors express their gratitude to JSC “Mangistaumunaigas” and LLP “KMG Engineering” for providing the opportunity to publish the results of this study.

References

American Petroleum Institute RECOMMENDED PRACTICE 63 (API RP 63), 1990. Recommended Practices for Evaluation of Polymers Used in Enhanced Oil Recovery Operations.

Hirasaki, G.J., and Pope, G.A. 1974. Analysis of Factors Influencing Mobility and Adsorption in the Flow of Polymer Solution Through Porous Media. *SPE J.* **14** (4): 337–346. https://doi.org/10.2118/4026-PA.

Jennings, R. R., Rogers, J. H. and West, T. J. 1971. Factors Influencing Mobility Control by Polymer Solutions. *J Pet Technol* **23** (3): 391-401. SPE-2867-PA. http://dx.doi.org/10.2118/2867-PA.

Leibin, E.L., Ogay E.K. 1979. Technological scheme of the Kalamkas field development. KazNIPIneft report, Shevchenko (in Russian).

Manichand, R.N., and Seright, R.S. 2014. Field vs Laboratory Polymer Retention Values for a Polymer Flood in the Tambaredjo Field. *SPE Res Eval & Eng*. **17**(3): 314-325. doi.org/10.2118/169027-PA.

Pye, D. J. 1964. Improved Secondary Recovery by Control of Water Mobility. *J Pet Technol* **16** (8): 911-916. SPE-845-PA. http://dx.doi.org/10.2118/845-PA.

Sagyndikov, M., Mukhambetov, B., Orynbasar, Y., Nurbulatov, A., Aidarbayev, S. 2018. Evaluation of Polymer Flooding Efficiency at brownfield development stage of giant Kalamkas oilfield, Western Kazakhstan. Paper presented at the SPE Annual Caspian Technical Conference and Exhibition held in Astana, Kazakhstan, 31st October – 2nd November 2018. SPE-192555-MS. https://doi.org/10.2118/192555-MS.

Sagyndikov, M., Seright., R.S., Kudaibergenov, S., and Ogay, E. 2022. Field Demonstration of the Impact of Fractures on HPAM Injectivity, Propagation and Degradation. *SPE Journal* **27**. SPE-208611-PA. https://doi:10.2118/208611-PA.

Seright, R.S., Fan, T., Wavrik, K., and Balaban, R.C. 2011. New Insights into Polymer Rheology in Porous Media. *SPE J.* **16** (1): 35-42. SPE-129200-PA. https://doi.org/10.2118/129200-PA.

Seright, R.S. 2017. How Much Polymer Should Be Injected During a Polymer Flood? Review of Previous and Current Practices. *SPE J*. **22** (1): 1-18. SPE-179543-PA. https://doi.org/10.2118/179543-PA.

Sheng, J., Leonhardt, B., Azri, N. Status of Polymer-Flooding Technology. 2015. *J Can Pet Technol* **54** (02): 116–126. SPE-174541-PA. https://doi.org/10.2118/174541-PA.

Smith, F. W. 1970. The Behavior of Partially Hydrolyzed Polyacrylamide Solutions in Porous Media. *J Pet Technol* **22** (2): 148-156. SPE-2422-PA. http://dx.doi.org/! 0.2118/2422-PA.

Wang, D., Li, C., & Seright, R.S. 2020. Laboratory Evaluation of Polymer Retention in a Heavy Oil Sand for a Polymer Flooding Application on Alaska's North Slope. *SPE Journal* **25**(4) 1842-1856. doi:10.2118/200428-PA.